CXCR4 signaling is controlled by immobilization at the plasma membrane

Beletkaia, E.; Fenz, S.F.; Pomp, W.; Snaar-Jagalska, B.E.; Hogendoorn, P.W.C.; Schmidt, T.

Biochimica et Biophysica Acta 1863 (2016) 607–616

Contents lists available at ScienceDirect

Biochimica et Biophysica Acta

journal homepage: www.elsevier.com/locate/bbamcr

CXCR4 signaling is controlled by immobilization at the plasma membrane

Elena Beletkaia [a], Susanne F. Fenz [d], Wim Pomp [a], B. Ewa Snaar-Jagalska [b], Pancras W.C. Hogendoorn [c], Thomas Schmidt [a,*]

[a] Kammerlingh Onnes-Huygens Laboratory, Leiden University, Niels Bohrweg 2, 2333 CA, Leiden, The Netherlands
[b] Leiden Institute of Biology, Leiden University, Leiden, The Netherlands
[c] Leiden University Medical Center, Leiden, The Netherlands
[d] Department of Cell and Developmental Biology, Biocenter, University of Würzburg, Germany

ARTICLE INFO

Article history:
Received 21 May 2015
Received in revised form 23 December 2015
Accepted 29 December 2015
Available online 31 December 2015

Keywords:
CXCR4
Single molecule
Signaling
Endocytosis

ABSTRACT

Understanding of the regulation mechanisms of CXCR4 signaling is essential for revealing its role in physiological and pathological processes. Though biochemical pathways following CXCR4 activation by its ligand CXCL12 are well established, knowledge about the receptor dynamics on the plasma membrane remains limited. Here we used Ewing sarcoma-derived cells to unravel the processes that are involved in regulating CXCR4 dynamics on the plasma membrane during receptor signaling. Single-molecule epi-fluorescence microscopy showed that CXCR4 was present in monomeric state on the plasma membrane independent of receptor stimulation. However, upon activation freely diffusing receptors were immobilized in a ligand concentration-dependent manner. CXCR4 immobilization was strongly correlated with the ability for G-protein signaling and was a precursor of subsequent endocytotic events. Our data suggest that, a balanced regulation of G-protein dependent and independent pathways is required for controlling CXCR4 receptor mobility, and potentially subsequent controlled signal transduction.

1. Introduction

Ewing sarcoma is a high-grade aggressive tumor occurring predominantly in bones of young children and adolescent. About a quarter of Ewing sarcoma patients have developed metastasis present at first diagnosis [23]. The characteristic and most common chromosomal translocation fusing a portion of the EWSR1 gene to the FLI gene, t(11;22)(q24;q12), results in the chimeric protein, EWS/FLI. This translocation was shown to change the expression of many different genes [23]. Frequently over-expressed in Ewing sarcoma is the chemokine receptor/ligand CXCR4/CXCL12 axis that was suggested to promote tumor progression and cell growth [3]. Additionally, CXCR4 was shown to be associated with Ewing sarcoma metastasis and with a poor prognosis for patients [2,19]. Thus, understanding of the molecular mechanisms of CXCR4 signaling regulation is essential.

The C-X-C motif chemokine receptor type 4 (CXCR4) belongs to the class of G-protein coupled receptor (GPCRs). CXCR4 selectively binds to the C-X-C chemokine CXCL12. The CXCR4/CXCL12 pathway is biochemically well studied [55]. Binding of CXCL12 causes conformational changes of the receptor and promotes activation of the G-protein hetero-trimer. Dissociation of the trimer into G_{α}- and $G_{\beta\gamma}$-subunits leads to initiation of the respective pathways downstream of CXCR4. CXCR4 activates four different G_{α} subunits [43] in turn mainly coupling to $G_{\alpha q}$ and $G_{\alpha i}$ [55]. Activation of $G_{\alpha q}$ regulates proteinkinase C (PKC) signaling that leads to Ca^{2+} release. The $G_{\alpha i}$-pathway involves activation of Akt, Erk1/2 and Cdc42 cascades. Dissociated $G_{\beta\gamma}$ activates phospholipase-C (PLC) and phosphoinositide-3 kinase (PI3K). The ultimate outcome of CXCR4 signaling leads to gene transcription, cell adhesion and cell migration [6,38,55] and hence can be involved in tumor, e.g. Ewing sarcoma, progression and metastasis.

Frequently GPCR signaling is controlled via receptor dimerization. There is evidence that CXCL12-induced activation of CXCR4 leads to the formation of heterodimers with CCR2 and CXCR7 [11,24,27,53]. It was shown that CXCR7 can regulate CXCR4-dependent pathways by promoting or inhibiting G-protein activation [11,24], or act as a CXCL12 scavenger [37]. However, some Ewing sarcoma cells, including cell line A673, do not express CXCR7 nor CCR2 to any significant level ([2,47]; see also table S1 in the supplemental material) such that heterodimerization with the latter is unlikely.

Many GPCRs are in a dynamic equilibrium between monomers and homo-dimers on the plasma membrane [18]. BRET experiments imply that a small portion of CXCR4 forms homodimers even in the absence of CXCL12 [14]. Additionally, the CXCR4 crystal structure suggests that

* Corresponding author.

http://dx.doi.org/10.1016/j.bbamcr.2015.12.020
0167-4889/

CXCR4 are homodimers [64]. Some studies report that stimulation with CXCL12 is required for CXCR4 homodimerization [53], while others report no dimerization of CXCR4 upon activation [14].

Along with receptor dimerization, internalization of GPCRs is considered a regulatory process. Upon activation CXCR4 promotes β-arrestin recruitment that subsequently leads to receptor internalization. Internalized receptors in turn can be recycled to the plasma membrane or follow the lysosomal path towards breakdown [6]. This process is recognized as receptor desensitization. In Ewing sarcoma endocytosis was identified to have a strong impact on receptor signaling [32]. Moreover, the main component of caveolin-dependent endocytosis, caveolin-1 is overexpressed in Ewing sarcoma [39] suggesting an important role of endocytosis in signal disregulation in these cells.

In summary, knowledge about CXCR4 dynamics on the plasma membrane is controversial. Hence, we decided to use the high spatial and temporal resolution that is combined in single-molecule microscopy to obtain novel understanding of CXCR4 signaling. In the last decade a number of single-molecule studies were undertaken to study receptor dynamics on the plasma membrane and relate the findings to the signaling outcome [7,10,17,25,58,66]. Here we investigated the membrane dynamics of CXCR4-eYFP in the Ewing sarcoma derived cell line A673 and followed receptor endocytosis on stimulation. We observed a correlation between receptor stimulation and mobility. Immobilization of the activated receptor was facilitated via clathrin-dependent endocytosis. Interestingly, we found indications that a regulatory cross-talk between G-protein dependent and independent pathways was acting in controlling regulation of CXCR4 signaling from the plasma membrane.

2. Results

2.1. CXCR4-eYFP is functional in A673-CXCR4 cells

We used the Ewing sarcoma-derived cell line A673 [31]. For fluorescence imaging of CXCR4 we stably transfected A673 wt cells with DNA encoding for CXCR4-eYFP (further referred to as A673-CXCR4 cells). We estimated the transfection efficiency to be ~50%. The transfected cells exhibited different expression levels of the CXCR4-eYFP construct. This mixed population of cells with high and low expression levels of CXCR4-eYFP, was advantageous given the different requirements of the respective experimental techniques. Where single-molecule imaging demanded a low density of the fluorescent molecules ($<1\ \mu m^{-2}$), other imaging techniques, in particular confocal microscopy, required substantially higher expression levels. The expression level of CXCR4-eYFP in A673-CXCR4 used for single molecule imaging was estimated as described in [10]. Briefly, the cell's membrane surface we approximated as a spheroid with a short axis of 20 μm and long axis of 50 μm yielding a cell surface area of $\sim 1.1 \times 10^3\ \mu m^2$. The fluorescence of CXCR4-eYFP at the apical membrane was detected when illuminated at 2 kW/cm^2 and 514 nm. The measured signal (35×10^3 cnts/pxl) was divided by the signal predicted for individual eYFP molecules under the same conditions, 220 cnts [15,16,59]. This calculation yielded an average expression level of $(4 \pm 1) \times 10^4$ CXCR4-eYFP molecules per cell, which is within the reported range of endogenous expressed GPCRs in mammalian cells [30]. Confocal microscopy showed that CXCR4-eYFP was primarily localized at the plasma membrane (Fig. 1A). CXCR4-eYFP was uniformly distributed and did not form any macroscopic domains (Fig. 1A left). The CXCR4-eYFP localized in the intracellular compartments in confocal imaging was presumably a result of overexpression.

To show that the CXCR4-eYFP was functional and that the fluorescent tag (eYFP) did not alter CXCR4 signaling, we performed functionality assays on A673-CXCR4 cells. First, we measured intracellular calcium release upon receptor stimulation using the Ca^{2+} reporter Fluo4-AM. Cells were pre-incubated with Fluo4-AM, and subsequently the change in fluorescence signal on global stimulation of the receptors with 100 nM CXCL12 was monitored for individual cells. The increase of the fluorescence intensity of Fluo4-AM corresponds to the increase of cytoplasmic Ca^{2+}. Fig. 1B shows a representative measurement of the change of fluorescence signal. The data shown were normalized to the signal before cell stimulation. Similar to the results reported earlier [36,61], stimulation with CXCL12 caused a calcium release, within 20 s. Cells expressing CXCR4-eYFP showed a 3.8 ± 0.3-fold intensity increase after receptor stimulation. This result indicates that CXCR4-eYFP were functional and capable of inducing Ca^{2+} release through the respective, $G_{\alpha q}$ and $G_{\alpha i}$-associated activation of the PLC-β pathway.

Another pathway activated shortly after receptor stimulation induces receptor endocytosis. Many GPCRs show internalization via clathrin-dependent endocytosis [61]. Some studies revealed, that upon stimulation CXCR4 internalizes 2 min after activation and reaches a maximum internalization level after ~30 min [41,61]. Therefore, we confirmed that CXCR4-eYFP behaved similarly using 2 min time-lapse confocal imaging after CXCL12 addition (Fig. 1C; Movie 1 in supplementary material). Endocytotic vesicles that contained the fluorescent receptor were manually counted in each frame. Fig. 1C shows, that after 20 min the number of vesicles increased significantly and reached a maximum after 40 min. The lack of internalization at an earlier time could be explained (1) by the fact that with confocal imaging only vesicles containing multiple copies of CXCR4-eYFP could be detected. (2) Only at a later time the newly formed vesicle detached from the plasma membrane had travelled far enough (~600 nm) to be distinguishable as entities inside the cell [20,52]. Our result confirmed that activation with CXCL12 leads to internalization of CXCR4-eYFP, presumably followed by concomitant activation of the β-arrestin pathway.

It should be noted that the migratory behavior of the A673-CXCR4 cells in a scratch assay was not altered when compared to the A673 wt cells (data not shown). Independent on stimulation with CXCL12, A673 cells showed only low migratory capacity.

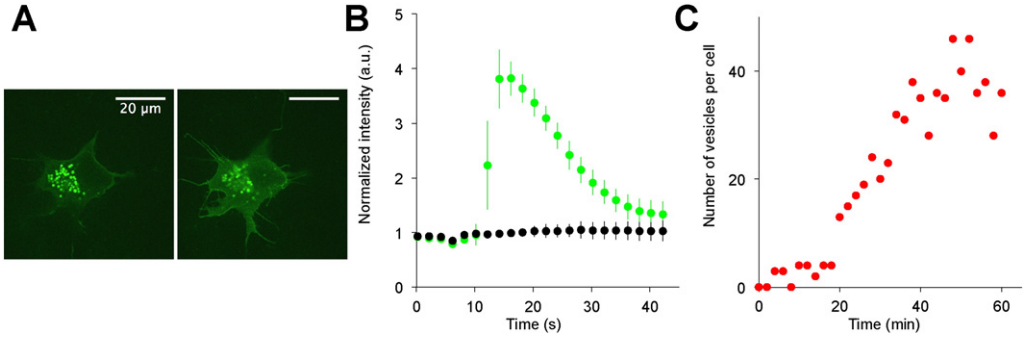

Fig. 1. *Characterization of the A673-CXCR4 cell line.* A. Confocal images of A673 cells stably transfected with CXCR4-eYFP. The images were acquired by focusing on the basal membrane (left) and in cytoplasmic cross-section of the cell (right). B. Exemplary Ca^{2+} assay measurement. The curves represent the change in fluorescence intensity of the Ca^{2+} indicator – Fluo4-AM – detected in non-transfected cells (black, n = 5) or cells transfected with CXCR4-eYFP (green, n = 3), after uniform stimulation with 100 nM CXCL12. The error bars represent the standard deviation. C. Appearance of the endocytotic vesicles containing CXCR4-eYFP detected within 60 min after cell stimulation with 100 nM CXCL12.

In summary, we showed that CXCR4-eYFP was properly localized, functional and did not alter the physiological response of the cells. Therefore, we concluded that the A673-CXCR4 cell line was suitable for the study of CXCR4 dynamics and to derive physiological effects.

2.2. CXCR4 do not homodimerize upon activation in A673 cells

The biochemical responses of CXCR4 upon stimulation are well established [55]. CXCL12 binding to CXCR4 facilitates conformational changes of the receptor leading to the activation of multiple pathways [55]. However, knowledge about a possible role in CXCR4 dimerization upon activation is still limited. Earlier reports showed that in 293T cells CXCR4 can be observed in a homo-dimeric configuration in resting cells and undergoes further homodimerization upon stimulation with CXCL12 [14,53,62]. To test for the presence of homo-dimers/multimers of CXCR4-eYFP in A673, we analyzed the signal strength of $>10^5$ signals that were detected on the plasma membrane of transfected cells with and without stimulation by CXCL12 (Fig. 2). For individual eYFP molecules at an illumination intensity of 2 kW/cm^2 at 514 nm and an illumination time of 5 ms we expected a signal of ~220 cnts for individual YPF-molecules [15,16,59]. The appearance of larger signals (>400 cnts) would indicate, that two or more eYFP molecules were detected within the same diffraction limited signal, therefore pointing to receptor dimers or multimers, respectively [7,34,49]. For resting cells (0 nM) the signal distribution showed only one peak with the maximum at ~200 cnts (Fig. 2), corresponding to CXCR4-eYFP monomers. The monomeric distribution did not change upon stimulation with various concentrations of CXCL12 up to 200 nM (Fig. 2), indicating that CXCR4 stayed monomeric even after activation.

In summary, CXCR4 is a monomeric protein on the plasma membrane of A673 cells independent of its activation state by CXCL12.

2.3. Activation of CXCR4 causes immobilization of the receptors

To get deeper insights into the behavior of CXCR4 on the plasma membrane and how it is regulated upon stimulation we applied single-molecule fluorescence microscopy and studied the diffusion dynamics of individual CXCR4-eYFP receptors on the millisecond time-scale at a position accuracy of $\sigma_{p.a.} = 35 \pm 7$ nm (Fig. S1). A 514 laser beam at 2 kW/cm^2 was used in the triggered mode (5 ms illumination) to acquire movies with 1500 frames at a frame-rate of 20 Hz. Each detected fluorescent signal was fit to a 2D-Gaussian (Fig. 3A) and filtered with respect to the previously determined eYFP footprint [59]. Subsequently, analysis by particle image correlation spectroscopy (PICS) [51] was applied to construct the cumulative probability density functions (cdfs) of square displacement for various time lags. Our results revealed that in resting cells the cdfs were best described with a model accounting for two fractions, a mobile receptor fraction and an immobile receptor fraction (Fig. S2A, green line). The fraction size (α) and mean square displacements (MSD_1 and MSD_2) were calculated according to Eq. (1) in M&M for various time lags from 50 ms up to 300 ms. The change of MSD_1 and MSD_2 varied with the time lag as shown in Fig. 3B. MSD_2 did not change over time and was equal to 0.013 ± 0.001 μm^2. It is important to note that the value of MSD_2 was significantly larger than that predicted for an immobile receptor of $4\sigma_{p.a.} = 0.005 \pm 0.001$ μm^2. This indicates that processes at a shorter time scale (<50 ms), which we could not detect with our imaging settings were responsible for this initial increase. Nonetheless, for brevity, we further refer to the receptor fraction with MSD_2 as immobile.

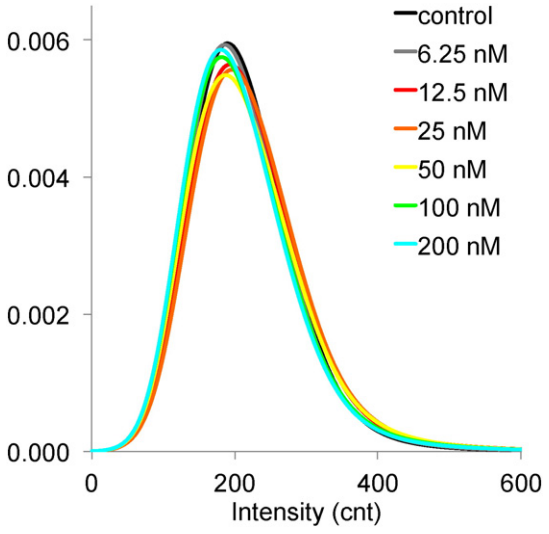

Fig. 2. Normalized probability density of the intensity of eYFP molecules collected during measurements with or without stimulation. Different colors represent different concentrations of CXCL12.

MSD_1 showed a linear dependence on the time lag as predicted for free diffusion (Fig. 3B). Fitting according to Eq (3) in M&M yielded $D_{CXCR4} = 0.18 \pm 0.01$ μm^2/s. This value is in good agreement with the diffusion coefficient determined, e.g. for the cAMP-receptor in Dictyostelium (0.17 ± 0.02 μm^2/s) [10] or other GPCRs in mammalian cells [7,25]. The fraction of mobile receptors comprised $\alpha = 81 \pm 3\%$ of the receptors.

To study how the activation of CXCR4 influences the behavior of the receptor on the plasma membrane, we applied global stimulation of the cells with CXCL12. CXCL12 was added to the cells right before imaging and single-molecule data were collected within the following hour. Up to five cells were imaged sequentially during one experiment. Each cell was taken as a representative of a 10–15 min time window after CXCL12 addition. At least 20 cells were imaged per condition. As shown in Fig. 3D the mobile receptor fraction size (α) detected for every individual cell during activation exhibited a similar value as for the following cells. The mobile receptor fraction determined from simultaneous analysis of all cells within the experiment (Fig. 3D, All) exhibited the same value as that of individual cells. This result suggests that receptor stimulation had a long-lasting effect on the receptor mobility and did not change over time within 60 min.

Our results showed a strong correlation between receptor stimulation and receptor mobility in a concentration-dependent manner. Addition of increasing concentrations of CXCL12 systematically shifted the cumulative probability distribution of square displacements to lower values (Fig. S2B). The shift in the cdf was attributed to a redistribution of the receptor fractions. As shown in Fig. 3C, the mobile receptor fraction decreased from ~80% (no CXCL12) to ~45% (200 nM CXCL12) in a CXCL12 concentrations-dependent manner. This finding was in agreement with earlier findings for other GPCRs [17,25]. It is noteworthy that an increase in receptor mobility has been found for cAMP-receptor in Dictyostelium [10] and for $GABA_B$ in HEK293 cells [7].

In summary, our results showed that CXCR4 on the plasma membrane is either freely diffusing or immobile. CXCR4 is immobilized upon stimulation with CXCL12 in a concentration-dependent manner.

2.4. Actin cytoskeleton is not responsible for CXCR4 immobilization

Many studies agree that GPCR dynamics is actin-cytoskeleton regulated [1,28,40,57]. Thus, we decided to test whether the actin cytoskeleton underlining the plasma membrane could be involved in modulation of CXCR4 mobility. For this purpose, we induced actin depolymerization by Latrunculin B (LatB). Pre-incubation with LatB for 30 min was sufficient to effectively deplete actin (Fig. S3). LatB induces only temporal actin-cytoskeleton depolymerization. We analyzed the data acquired within the first 30 min after medium exchange, while the data collected at 30–60 min after which the membrane-skeleton was re-established served as a control.

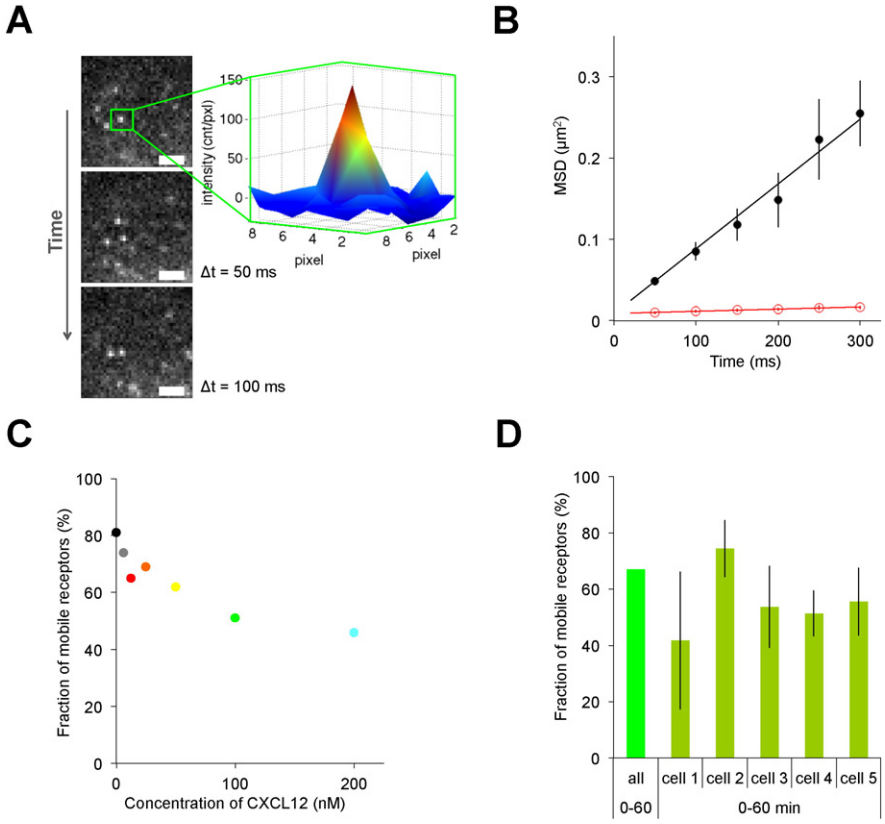

Fig. 3. *Single-molecule characterization of CXCR4 diffusion in resting cells and upon global stimulation with CXCL12.* A. Single-molecule imaging scheme. Scale-bar: 2 μm. B. Mean square displacement (MSD) vs time plot. MSD of mobile (blue) and immobile (purple) receptors as resulting from a simultaneous fit of the resting and CXCL12 stimulated cells' data sets. C. Dependence of the mobile receptor fraction on the CXCL12 concentration. The color-code corresponds to the one used in Fig. 2. D. The mobile receptor fraction detected at different time points after addition of 100 nM CXCL12 within one experiment. Cell1–cell5 represents five individual cells imaged subsequently within one experiment (0–60 min). 'All' represent the mobile receptor fraction detected by simultaneous analysis of all cells imaged within one experiment.

To our surprise actin depolymerization did not lead to an increase of the mobile receptor fraction but rather to a decrease to ~61% (Fig. 4A, 0–30 min) in non-stimulated cells. Receptor activation with 100 nM CXCL12 slightly changed the mobile receptor fraction to 69% (Fig. 4A, 0–30 min). Data collected after actin repolymerization (30 min after medium exchange) replicated the results acquired for cells with intact actin cytoskeleton (Fig. 4A, 30–60 min). In resting cells, the fraction of the mobile receptors reached 77% and in the cells stimulated with CXCL12, it dropped to 56%.

In summary, our results suggest that in resting cells with intact actin skeleton, the immobile CXCR4 receptors were not anchored to the actin cytoskeleton. Activation by CXCL12 induced an actin-dependent process promoting CXCR4 immobilization. Thus, our result suggests that actin might have an indirect effect on CXCR4 regulation, which will be discussed later.

2.5. CXCR4 in endocytotic vesicles contribute to the immobile receptor fraction

Upon stimulation many GPCRs proceed to internalization [50,55,57]. Activated GPCRs are known to bind to β-arrestin, which in turn links them to the AP2 adapter complex [60] and facilitates their clathrin-dependent endocytosis. Given that CXCR4 is known to internalize via clathrin-dependent endocytosis upon stimulation and, at the same time, to undergo constitutive internalization without stimulation [4], we further hypothesized that receptor internalization could possibly explain the drop of the mobile CXCR4 receptor fraction upon stimulation.

To test this hypothesis we inhibited clathrin-mediated endocytosis by the water-soluble inhibitor chlorpromazine (CHZ). CHZ causes loss of clathrin from the cell surface in the coated pits and, therefore, prevents formation of new clathrin-coated vesicles (CCVs) [54,63]. 30 min incubation of A673-CXCR4 cells with 25 μM CHZ was sufficient to inhibit clathrin-dependent endocytosis of CXCR4 effectively.

Single-molecule imaging revealed that CHZ pre-treated cells exhibited the same mobile CXCR4 receptor fraction ($\alpha = 74 \pm 9\%$) as control cells ($\alpha = 81 \pm 3\%$). However, in the CHZ pre-treated cells the mobile receptor fraction was composed of two sub-fractions, a freely diffusing fraction ($62 \pm 7\%$) and a receptor fraction that exhibited confined diffusion ($12 \pm 9\%$). The latter is reflected by a sub-linear increase of MSD with timelag (Fig. 4 B,C). Both sub-fractions of mobile receptors showed similar diffusion coefficients as the fraction of mobile receptors in resting cells, $D^{(CHZ)}_{CXCR4} = 0.16 \pm 0.02\ \mu m^2/s$. The size of the confinement zone was estimated from a fit to the plateau in the MSD vs time plot (Fig. 4B) according to Eq. (4) in M&M and yielded $r_{conf} = 236 \pm 6$ nm.

Given the typical radius of a clathrin-coated vesicle of ~75–100 nm [33], which contains a surface area of 0.07–0.13 μm^2, equal to the area covered by the confinement zone in our experiments, we suggest that receptors exhibiting confined diffusion correspond to the receptors trapped in a pre-cursor structure of clathrin-coated pits. Thus, in CHZ pre-treated cells mobile receptors undergoing constitutive internalization accumulate in a precursor structure of clathrin-coated pits and stay locked there since endocytosis cannot proceed.

When CHZ pre-treated cells were stimulated with 100 nM CXCL12, the fraction of mobile receptors decreased ($\alpha = 56 \pm 6\%$) and the distribution of receptors between freely diffusing and confined fractions changed dramatically (Fig. 4C). Nearly all receptors showed confined diffusion, while only a small fraction showed free diffusion ($52 \pm 5\%$

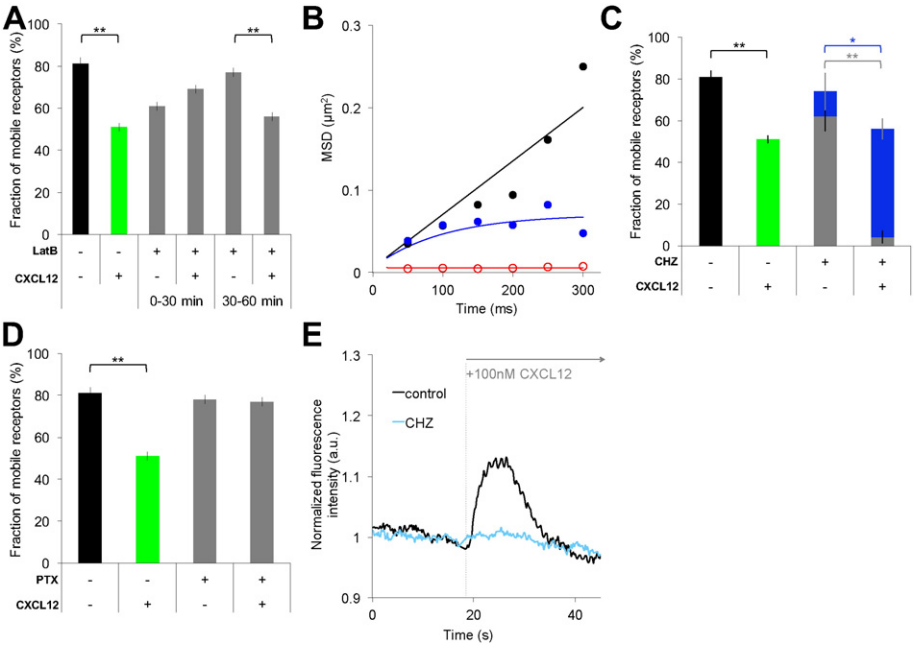

Fig. 4. *Effect of different drug treatments.* A. The fraction of mobile CXCR4-eYFP in cells pre-treated with LatB (grey) without or with global stimulation by 100 nM CXCL12, compared to the mobile receptor fraction measured in control cells without (black) and with (green) stimulation. LatB provided temporal actin depletion, therefore the acquired data was split accordingly: 0–30 min and 30–60 min. B. The MSD vs. time plot of the immobile (red), confined (blue) and freely mobile (black) receptors measured in CHZ pre-treated cells. Solid lines represent the respective fit of the data. The linear size of the confinement zone was estimated from the linear fit to the plateau and yielded $r_{conf} = 236 \pm 6$ nm. C. The mobile receptor fraction in CHZ treated cells presented by two sub-fractions of mobile receptors: freely diffusing (grey) and confined (blue). Uniform admission of 100 nM CXCL12 caused a drastic change in the ratio of mobile subpopulations. The total size of the mobile fraction in CHZ pre-treated cells was comparable to the one in the control cells without (black) or with (green) CXCL12 admission. D. Fraction of mobile CXCR4-eYFP measured in PTX pre-treated (purple) cells without and with (green punctate pattern) activation, compared to control cells without (black) and with (green) uniform stimulation with 100 nM CXCL12. E. Ca^{2+} assay. The curves represent the change in fluorescence intensity of the Ca^{2+} indicator – Fluo4-AM – detected in cells pre-treated with chlorpromazine (CHZ, light blue) or in control (black) cells after uniform stimulation with 100 nM CXCL12. (significance levels: *: $p < 0.01$ and **: for $p < 0.001$).

and 4 ± 3%, respectively), suggesting that activated receptors proceed to internalization. This is in good agreement with our internalization experiment (Fig. 1C) and with data from other groups [41,61], showing that upon stimulation the rate of CXCR4 internalization increases.

It has been reported that CHZ, like other endocytosis inhibitors, exhibit physiological side effects [12]. Hence, we performed additional studies using the endocytosis inhibitor pitstop 2. Pitstop specifically targets clathrin-mediated endocytosis via interference with the terminal domain of the clathrin heavy chain [22]. Qualitatively the experiments retrieved the results we obtained with CHZ. We found a confined-diffusion fraction characterized by a confinement size of 220 nm. Receptor stimulation with 100 nM CXCL12 led to some receptor redistribution between fractions, but less dramatic as that we found for CHZ treatment (Fig. S4). A quantitative agreement could not be obtained, given the significant effect that even lowest concentrations of the pitstop-solvent DMSO has on membrane mobility [13,26].

In summary, CHZ prevents the formation of clathrin-coated vesicles and, hence, receptors proceeding to internalization get trapped in confined areas reminiscent of precursor structures of coated pits. Taken that, the fraction of the immobile receptors increased upon stimulation, our results suggest, that receptor immobilization was only partially caused by CXCR4 capture to clathrin-coated vesicles. The size of those vesicles was too small to directly observe receptor diffusion in the vesicle membrane (see below).

2.6. G-proteins control CXCR4 immobilization

Up to date, internalization of GPCR's is considered as a way of receptor desensitization. Our results, suggest that internalizing receptors appears as immobile. At the same time we find that immobilization of CXCR4 correlated with activation of receptors. Therefore, having established a correlation between receptor mobility and signaling, we were interested in how receptor mobility is affected when the signaling chain is disrupted at the level of G-proteins. Previous reports showed a change in G-protein mobility while the cAR1 receptor was stimulated [59]. Stimulation of CXCR4 mainly results in activation of two isoforms of the G_α subunit: $G_{\alpha q}$ and $G_{\alpha i}$ [55]. Kleemann et al. showed elevated coupling of $G_{\alpha i}$ to CXCR4 upon receptor stimulation [21]. This coupling of the $G_{\alpha i}$ on the cytosolic side should not per se influence the receptor dynamics. However, hypothesizing that the $G_{\alpha i}$ pathway activation might result in formation of a supramolecular scaffold [42] for further signaling, we probed how the interaction of CXCR4 with the $G_{\alpha i}$ subunit could modulate the mobile receptor fraction.

In our experiments we used pertussis toxin (PTX) as an agent resulting in loss of coupling of $G_{\alpha i}$ and the receptor [29,35]. We pre-incubated A673-CXCR4 cells with PTX for 5 h. During the experiments PXT was also present in the medium. As predicted, in the resting cells, single-molecule imaging of CXCR4-eYFP did not show any change in the diffusion coefficient of the receptors. Moreover, the mobile receptor fraction did not change compared to the control without PXT (Fig. 4D), suggesting that if $G_{\alpha i}$ was coupled to CXCR4 it had no measurable impact on the receptor dynamics. However, when 100 nM CXCL12 was added to the cells, no significant drop in the mobile receptor fraction was observed (Fig. 4D). This behavior was in contrast to the decrease in the mobile receptor fraction detected for CXCR4 receptors upon stimulation in control cells (Fig. 4D, green bar). This result supports our earlier conclusion that a bigger fraction of immobile receptors is strongly correlated to receptor signaling.

In summary, our results imply that the decrease in the mobile receptor fraction upon stimulation must be interpreted as an outcome of the of the subsequent $G_{\alpha i}$-pathway activation potentially resulting in formation of a supramolecular scaffold (signalosome, Fig. 5), while blocking the receptor interaction with $G_{\alpha i}$ lead to receptor mobility that did not change upon stimulation.

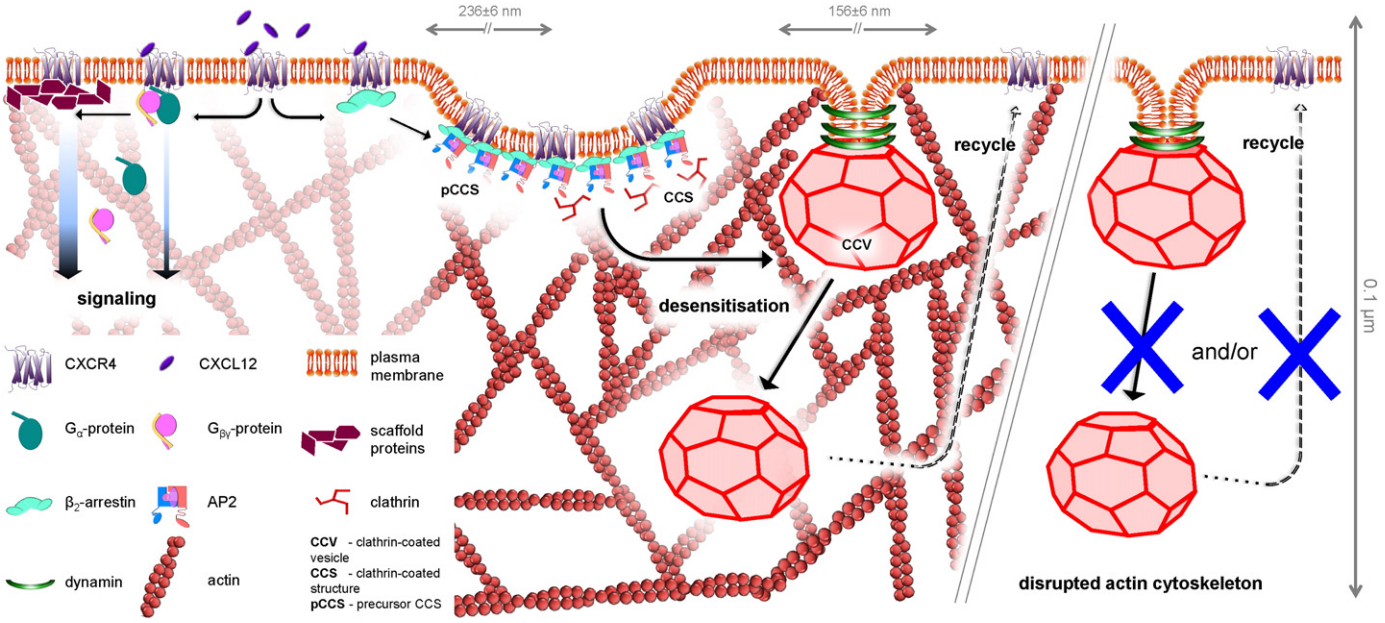

Fig. 5. *Model.* Binding with CXCL12 CXCR4 is activating G-protein dependent (left) and independent (right) pathways. Activation of the biochemical pathways results in CXCR4 immobilization either in super-molecular signalosome, causing enhanced signaling, or in the clathrin-coated vesicles, resulting in receptor internalization, imply a cross-talk between these signaling cascades.

2.7. Cross-talk between G-protein dependent and independent pathways

Our results showed, that immobilization of CXCR4 upon stimulation is facilitated via receptor endocytosis. At the same time the $G_{\alpha i}$-dependent pathway also leads to CXCR4 immobilization. Taken together, these results suggest that G-protein dependent and independent pathways are cross-regulated. Thus, we checked whether a G-protein dependent pathway would be affected by inhibition of CXCR4 endocytosis. We performed a Ca^{2+} assay with the cells under different conditions. Cells with inhibited clathrin-dependent endocytosis (pre-treated with CHZ) showed no Ca^{2+} release upon CXCR4 activation (Fig. 4E). This result implies, that the G-protein independent pathway of receptor internalization was interfering with the early stages of a G_α-dependent pathway.

In summary, we suggest that two processes together regulate CXCR4 mobility and, thus, activation/signaling. Endocytosis driven immobilization leads to desensitization while G-protein driven local signalosome formation might result in signal enhancement (Fig. 5). Together, both processes regulate the overall cellular response.

3. Discussion

GPCR signaling is a complex process in which only parts have been unraveled. Activation of CXCR4 promotes signaling through G-proteins resulting in expression of certain genes, cells survival/proliferation, chemotaxis, etc. Simultaneously G-protein independent pathways, e.g. β-arrestin, are activated and result in receptor desensitization [55]. All the biochemical pathways are studied in detail, but the role of the receptor dynamics on the plasma membrane remains poorly understood.

To elucidate the molecular mechanism of CXCR4 signal transduction, we studied CXCR4 during activation using the receptor mobility as a marker. Our results revealed that already in the resting cells receptor diffusion was not homogeneous. We detected two receptor species, one mobile and one immobile. Activation of CXCR4 with CXCL12 caused a concentration-dependent decrease of the mobile receptor fraction, indicating a correlation between receptor signaling and diffusion on the plasma membrane. Our data gives information on receptor diffusion at millisecond time scales, while, most biochemical or other receptor-signaling processes require longer time, e.g. endocytosis of a receptor takes ~1 min [5,9]. In this respect, our results depict a snapshot of the overall processes. However, we did not observe a time dependent change in the mobile receptor fraction (Fig. 3D), meaning that there was a constitutive fraction of immobile receptors.

Many studies of GPCRs agree that receptors behavior/signaling strongly depends on the actin cytoskeleton. Actin remodeling was reported to have a key role in the pro-apoptotic responses upon GPCR activation [40]. Luo et al. showed that a major portion of CXCR4 is pre-coupled with the cortical actin binding protein – cortactin [28]. Stimulation with CXCL12 induces further translocation of cortactin from endosomal compartments and colocalization with CXCR4. However, our results did not show actin-dependent changes in the diffusion coefficient of CXCR4, and actin depletion did not cause the predicted increase in receptor mobility. In contrast, in the actin depleted cells the fraction of mobile receptors was decreased compared to the control. These results imply that there is no direct physical interaction between receptors and actin. However, the change in the CXCR4 mobile fraction indicated, that there was actin-dependent regulation of receptor mobility.

Actin is known to play an important role in sorting of GPCRs to diverse membrane pathways after endocytosis [46,57]. For instance, linking of the β2-adrenoreceptor to actin inhibits trafficking of endocytosed receptors to lysosomes and promotes their recycling to the plasma membrane [57]. Therefore, during actin cytoskeleton depletion one could expect that most of the receptors, which are endocytosed, follow the lysosomal route instead of being recycled to the plasma membrane (Fig. 5, right side). Such a process could lead to a change in the balance of different fractions of receptors present on the plasma membrane. Moreover, there are indications that actin is involved in all forms of endocytosis [46]. Though, actin was reported to function as a late component of clathrin-dependent endocytosis [33] it is responsible for a range of processes [20]. EM imaging and life-cell imaging showed that depletion of the actin cytoskeleton caused an increased fraction of shallow and curved clathrin-coated structures on the plasma membrane in comparison to invaginated structures and formed vesicles [5,65]. Furthermore, it was shown that actin polymerization at the plasma membrane controls both the alignment and mobility of clathrin-coated vesicles, facilitates the internalization step,

and drives rapid transport of early endosomes away from the plasma membrane in the cytosol [46]. Hence, actin depletion can be considered as one form of indirect clathrin-dependent endocytosis inhibition at a later stage. Accordingly, in actin-depleted resting cells, CXCR4 undergoing constitutive internalization stall in vesicles, which cannot be removed from the plasma membrane (Fig. 5, right side). These receptors contribute to the observed immobile fraction (see below). During receptor activation, disturbed vesicle formation and/or vesicle scission could result in CXCR4 failing to proceed with endocytosis and to show the accompanying decrease in the mobile receptor fraction.

In our experiments we used chlorpromazine (CHZ) as water-soluble inhibitor of the clathrin-mediated endocytosis to directly address the question of how endocytosis interferes with the mobility of CXCR4 on the plasma membrane. CHZ causes loss of clathrin from the cell surface in the coated pits and, therefore, prevents formation of new clathrin-coated vesicles (CCVs) [54,63]. However, loss of clathrin from the cell surface would not affect the early stages of clathrin-coated structure (CCS) formation. Clathrin-coated vesicle formation consists of five steps: (1) nucleation, (2) cargo selection, (3) coat assembly, (4) scission and (5) uncoating [33]. The first two steps are promoted by a number of initiation proteins, e.g. FCHO 1,2, Epsin and adaptor proteins, e.g. β-arrestin. These proteins result in initiation of the membrane curvature and receptor recruitment (Fig. 5, middle). Further, the AP2 adaptor protein and clathrin are recruited during clathrin-coated pit maturation and coat assembly. Thus, a membrane invagination appears and progresses before recruitment of clathrin [33]. Therefore, CHZ pre-treated cells could still form precursor structures of clathrin-coated pits (pCCS).

Our data showed, that inhibition of a clathrin-dependent endocytosis with CHZ caused appearance of a receptor fraction undergoing confined diffusion. During CXCR4 activation in CHZ pre-treated cells all mobile receptors were diffusing in a confinement zone. The radius of the confinement zone (236 ± 6 nm) suggested that the confinement corresponded to precursor CCS (pCCS). Upon stimulation CXCR4 was driven to CCVs, but due to the CHZ pre-treatment, the receptors were confined to pCCS.

Thus, in untreated cells CXCR4 would be trapped in CCVs after stimulation. As the typical size of a CCV equals 100–200 nm which is within the axial resolution of our microscope (~1 μm), diffusion of the receptors on the vesicle surface will be detected as a 2D projection (Fig. 5). To elucidate the effect hereof, we modeled free diffusion of the receptor on a vesicle (see in M&M) with a diffusion coefficient $D_{CXCR4}^{(vesicle)} = 0.2\ \mu m^2/s$ on the surface of a vesicle with a diameter $d_{vesicle} = 150$ nm and subsequently analyzed the 2D-projection of the data. Our simulations revealed, that the $MSD_{sphere\text{-}2D}$ linearly increased with timelag and reached a plateau at a timelag of t = 50 ms (Fig. S5), which corresponds to the time lag of our single-molecule measurements. The simulations further revealed that the plateau value is given by $MSD_{sphere-2D}(t=\infty) = \frac{4}{3}R^2$, where R is the vesicle radius. Further, taking into account the positional accuracy of $\sigma_{p.a.} = 35 \pm 7$ nm, and the value we found for MSD_2, $\sigma_{MSD2} = 57 \pm 2$ nm, the vesicle radius is then given by $\frac{4}{3}R_{MSD2}^2 = 4\sigma_{MSD2}^2 - 4\sigma_{p.a.}^2$. Using our experimental findings we calculated a value $R_{MSD2} = 78 \pm 3$ nm which is very similar to the size of a clathrin-coated vesicle. Together these findings showed that the immobile receptors can be attributed to receptors diffusing in CCVs. Thus, CXCR4 undergoing constitutive internalization [4] would contribute to the immobile receptor fraction in resting cells and the increase of the immobile fraction during activation would be related to an elevated level of clathrin-dependent endocytosis of CXCR4. In summary, clathrin-dependent endocytosis is involved in regulation of CXCR4 mobility on the plasma membrane.

Stimulation experiments showed a concentration-dependent decrease of the mobile receptor fraction, indicating that receptor immobilization was correlated with CXCR4 activation. This was further confirmed by experiments in cells treated with PTX. PTX causes physical detachment of $G_{\alpha i}$ from CXCR4 resulting in arrested signaling. Detachment of $G_{\alpha i}$ from CXCR4 altered the ratio of mobile to immobile receptors in response to CXCL12 stimulation, compared to non-treated cells. There was no decrease in the mobile receptor fraction, further supporting our hypothesis of correlated CXCR4 mobility on the plasma membrane and signaling. As clathrin-dependent endocytosis is G-protein independent and the majority of biochemical signaling of CXCR4 is mediated through activation of the $G_{\alpha i}$-subunit, PTX is a tool to separate G-protein dependent and independent pathways. In contrast to neuroblastoma cells, where $G_{\alpha i}$ detachment with PTX failed to inhibit internalization of CXCR4 upon CXCL12 addition [8], our experiments suggest that in Ewing sarcoma, disrupted receptor signaling prevented receptor internalization. This idea is supported by a number of reports which showed an important role of caveolin (main component of caveolin-dependent endocytosis [39]) in signaling of various molecules in Ewing sarcoma [32,44,45,56]. For instance, it was shown that in Ewing sarcoma cells blockade of IGF1R endocytosis inhibits the receptor's signaling [32]. Furthermore, in our experiments, CHZ pre-treatment disturbed $G_{\alpha q}$-dependent Ca^{2+} release upon CXCL12 stimulation.

In conclusion, here we showed that in Ewing sarcoma derived A673 cells the CXCR4 receptor mobility on the plasma membrane is strongly correlated with receptor signaling. Activated receptors are immobilized into various structures on the plasma membrane. Immobilization of the receptor is facilitated via clathrin-dependent endocytosis structures, e.g. vesicles as well as via $G_{\alpha i}$ – initiated supramolecular scaffolding. Inasmuch as these processes lead to opposite effects (desensitization and signal enhancement in signalosomes, respectively) our results imply that a balanced and functional cross-talk of the G-protein dependent and independent pathways might be important for a faithful distribution of the mobile an immobile CXCR4 on the plasma membrane, which in turn might serve as a regulatory mechanism in receptor signal transduction.

4. Materials and methods

4.1. Cell culture and transfection

A673 cells were maintained in IMDM cell culture medium (Gibco, USA) supplemented with 10% fetal bovine serum (FBS, Gibco, USA) at 37 °C and 5% CO_2. To study the CXCR4 receptor, A673 wild type (A673 wt) cells were stably transfected using a retroviral construct encoding for CXCR4-eYFP (kindly provided by Prof. Dr. Nikolaus Heveker, University of Montreal). Viral transfection was performed as follows. 5×10^4 cells/well were seeded in a 24-well plate; the next day, 1MOI of viral particles and 5 μg/mL polybreen was added for 24 h, followed by medium refreshment. For experiments A673 cells stably transfected with CXCR4-eYFP (further referred to as A673-CXCR4 cells) were used after three passages.

4.2. Sample preparation

For imaging ~1×10^5 of A673-CXCR4 cells were placed in 0.35 mm culture dishes (Ibidi, Germany) in 2 mL of complete IMDM medium (with 10% FBS) and left to attach overnight. Before imaging the medium in the dish was replaced with fresh IMDM without serum to minimize autofluorescence. During imaging the CO_2 level was maintained at 5% and temperature at 37 °C using the INUBG2E-ZILCS (TokaiHit, Japan).

4.3. Global CXCL12 stimulation assay

Activation of the CXCR4 receptor with its specific ligand – CXCL12 (Gibco, USA) – was done as global stimulation just before imaging: CXCL12 was added to the medium to a final concentration of 6–200 nM. Single-molecule or confocal imaging was performed within 1 h after addition of CXCL12.

4.4. Calcium assay

The change of the intracellular Ca^{2+} concentration was measured using cell-permeant Fluo4-AM (Invitrogen, USA). Cells were supplemented with 10 μM Fluo4-AM for 30 min; prior to imaging the medium in the samples was replaced with fresh IMDM without serum to remove Fluo4-AM from the cells environment. Using time-lapse confocal microscopy (see below) the Fluo4-AM fluorescence was detected in individual cells with 50 ms laser pulses at 488 nm. Time-lapse imaging of the cells was done with a 100× objective at 5 Hz for 5 min. Where indicated, imaging was done with a 10× objective and the fluorescence change was determined for the whole field of view. At a specified time point 100 nM CXCL12 was added and the change in fluorescence intensity inside individual cells was registered.

4.5. Actin depolymerization

To induce cytoskeletal actin depolymerization cells were pre-incubated with 500 nM latrunculin B (LatB; Sigma, USA) for 30 min, which was sufficient for temporal actin cytoskeleton depletion. Subsequently cells were washed with fresh medium and imaged in serum free IMDM with or without global stimulation. Imaging was performed in a 30 min time window after medium change. The actin cytoskeleton was repolymerized within that time (Fig S1).

4.6. Endocytosis inhibition

Endocytosis inhibition was achieved by addition of 25 μM chlorpromazine (CHZ; Sigma, USA), to the cells for 30 min prior to imaging. For imaging the medium was replaced by serum free IMDM and single-molecule or confocal imaging was done in absence or presence of CXCL12.

4.7. $G_{\alpha i}$ inhibition

Pertussis toxin (PTX; Sigma, USA) was used to detach $G_{\alpha i}$ from CXCR4. A673-CXCR4 cells were pre-incubated with 200 ng/mL PTx for 5 h and then single-molecule imaging was done in presence of PTx in the serum free IMDM medium with or without global stimulation.

4.8. Single-molecule imaging

For single-molecule imaging we combined wide-field microscopy with high-sensitivity fluorescence microscopy as described in detail earlier [49]. In brief, the sample was mounted onto an inverted microscope (Zeiss, Germany) equipped with a 100× objective (NA = 1.4, Zeiss) and a liquid nitrogen-cooled back-illuminated CCD-camera (Princeton Instruments, USA). A region of interest was set to 40 × 40 pixels with an apparent pixel size of 202 ± 2 nm. Measurements were done by illumination of the sample with a 514 nm laser beam (Coherent, Germany) for 5 ms at the intensity of 2 kW/cm^2. 1500 images were recorded at 20 Hz. Use of the appropriate filter combination: dichroic: z405/514/647/1064rpc and emission filter: z514/647m (Chroma, USA) permitted the signal detection by the CCD-camera. The x/y positions of individual molecules was determined with a localization precision of $\sigma_{p.a.} = 35 \pm 7$ nm.

Image analysis was done using programs written in MatLab (Mathworks Inc., USA) as described before [49]. Briefly, the signal acquired from individual eYFP molecules was fitted with a 2D-Gaussian and filtered with respect to peak intensity, peak width and detection error thresholds. Subsequently, particle image-correlation spectroscopy analysis, PICS, [51] was used to calculate the cumulative probability (cdf) of squared displacements. The cdf revealed that CXCR4 diffusion was not homogeneous and was best described with a model accounting for two or three fractions:

$$\mathrm{cd}f_{2\mathrm{fr}}(r^2,t) = 1-\left(\alpha\cdot exp\left(-\frac{r^2}{\mathrm{MSD}_1(t)}\right)+(1-\alpha)\cdot exp\left(-\frac{r^2}{\mathrm{MSD}_2(t)}\right)\right) \quad (1)$$

$$\mathrm{cd}f_{3\mathrm{fr}}(r^2,t) = 1-\left(\alpha_1\cdot exp\left(-\frac{r^2}{\mathrm{MSD}_1(t)}\right)+\alpha_2\cdot exp\left(-\frac{r^2}{\mathrm{MSD}_2(t)}\right)+(1-\alpha_1-\alpha_2)\cdot exp\left(-\frac{r^2}{\mathrm{MSD}_3 t}\right)\right) \quad (2)$$

where α is the fraction size of the receptors with corresponding characteristic mean square displacement, MSD(t). The MSD(t) was calculated for different time lags, t, up to 300 ms. Subsequently the MSD was analyzed at different time lags to extract the diffusion coefficient (D):

$$\mathrm{MSD}(t_{\mathrm{lag}}) = 4Dt_{\mathrm{lag}} + s_0 \quad (3)$$

where the offset s_0 is a measure for the localization precision ($s_0 = 4\sigma^2$).

For each experimental condition the MSD and α was calculated separately. There was no difference in MSD values between resting and stimulated cells. Thus the data was re-analyzed jointly, with α as a free parameter.

In indicated cases the radius of the confinement, r_{conf}, was calculated as [48]:

$$MSD(t=\infty) = r_{conf}^2 + s_0 \quad (4)$$

4.9. Time-lapse microscopy

Time-lapse microscopy was performed using a spinning disk (Yokogawa, Japan) microscope (Zeiss, Germany) equipped with a motorized stage (Maerzhauser, Germany) and a home-built autofocus system facilitating time-lapse imaging at multiple positions. Imaging was done with a 10× or 100× objective (Zeiss, Germany) using brightfield, 488 nm or 514 nm laser illumination at a specified time lag. Image analysis was done using algorithms in MatLab (Mathworks Inc., USA).

4.10. Simulation of diffusion on a vesicle

We modeled free diffusion of the receptors with a diffusion coefficient $D_{CXCR4\ (vesicle)} = 0.2\ \mu m^2/s$ on the surface of a sphere with a diameter $d_{vesicle} = 150$ nm. Molecules on the sphere were initialised at the positions $\mathbf{p_i} = (x_i, y_i, z_i)$ representing a random distribution on the sphere surface. At each time-lag ($\Delta t = 10^{-5}$ s) each molecule was displaced to a temporary position $\mathbf{p_i'} = (x_i' = x_i + \Delta x_i, y_i' = y_i + \Delta y_i, z_i' = z_i + \Delta z_i)$. The displacement in each dimension, i.e. Δx_i, Δy_i and Δz_i, were assigned an arbitrary length randomly selected from a normal distribution with a width of $\sqrt{\mathrm{MSD}} = \sqrt{(2Dt)}$. On this scale the surface of the sphere was considered flat and the displacement of the molecule was taken as a projection of $\mathbf{p_i'}$ on the sphere surface by transformation into spherical coordinates, while the r-coordinate was set as equal to the radius of the sphere. Subsequently the new (x_i, y_i, z_i) positions of the molecules were determined as a transformation into cartesian coordinates. Thus, the (x_i, y_i, z_i) positions determined after each Δt represent the displacement of a molecule on the sphere surface. Using the (x_i, y_i) coordinates we calculated the mean square displacement of the molecules in a projection to a plane to mimic the image of moving molecules in a microscope image; $\mathrm{MSD}_{\mathrm{sphere\text{-}2D}}$. Our simulations revealed,

that at t = 50 ms $MSD_{sphere\text{-}2D}$ was reaching a plateau and the value of the plateau was determined to be:

$$lim_{t\to\infty} MSD_{sphere-2D}(t) = \frac{4}{3}R^2_{sphere}. \quad (5)$$

Transparency document

The Transparency document associated with this article can be found, in online version.

Acknowledgment

We thank S. Coppola for the help with the data analysis, Karoly Szuhai and Laurens Sand for the valuable comments on data interpretation. This work is part of the research program of the Netherlands Organization for Scientific Research (NWO), TOPGO.L.10.064. S. F. was funded from the grant No. 253755 in the programme FP7-PEOPLE-2009-IEF.

Appendix A. Supplementary data

Supplementary data to this article can be found online at http://dx.doi.org/10.1016/j.bbamcr.2015.12.020.

References

[1] N.L. Andrews, K.A. Lidke, J.R. Pfeiffer, A.R. Burns, B.S. Wilson, J.M. Oliver, D.S. Lidke, Actin restricts FcepsilonRI diffusion and facilitates antigen-induced receptor immobilization, Nat. Cell Biol. 10 (2008) 955–963.
[2] I.M. Bennani-Baiti, A. Cooper, E.R. Lawlor, M. Kauer, J. Ban, D.N. Aryee, H. Kovar, Intercohort gene expression co-analysis reveals chemokine receptors as prognostic indicators in Ewing's sarcoma, Clin. Cancer Res. 16 (2010) 3769–3778.
[3] D. Berghuis, M.W. Schilham, S.J. Santos, S. Savola, H.J. Knowles, U. Dirksen, K.L. Schaefer, J. Vakkila, P.C. Hogendoorn, A.C. Lankester, The CXCR4–CXCL12 axis in Ewing sarcoma: promotion of tumor growth rather than metastatic disease, Clin. Sarcoma Res. 2 (2012) 24.
[4] D. Bhandari, J. Trejo, J.L. Benovic, A. Marchese, Arrestin-2 interacts with the ubiquitin-protein isopeptide ligase atrophin-interacting protein 4 and mediates endosomal sorting of the chemokine receptor CXCR4, J. Biol. Chem. 282 (2007) 36971–36979.
[5] S. Boulant, C. Kural, J.C. Zeeh, F. Ubelmann, T. Kirchhausen, Actin dynamics counteract membrane tension during clathrin-mediated endocytosis, Nat. Cell Biol. 13 (2011) 1124–1131.
[6] J.M. Busillo, J.L. Benovic, Regulation of CXCR4 signaling, Biochim. Biophys. Acta 1768 (2007) 952–963.
[7] D. Calebiro, F. Rieken, J. Wagner, T. Sungkaworn, U. Zabel, A. Borzi, E. Cocucci, A. Zürn, M.J. Lohse, Single-molecule analysis of fluorescently labeled G-protein-coupled receptors reveals complexes with distinct dynamics and organization, Proc. Natl. Acad. Sci. U. S. A. 110 (2013) 743–748.
[8] I.C. Clift, A.O. Bamidele, C. Rodriguez-Ramirez, K.N. Kremer, K.E. Hedin, β-Arrestin1 and distinct CXCR4 structures are required for stromal derived factor-1 to downregulate CXCR4 cell-surface levels in neuroblastoma, Mol. Pharmacol. 85 (2014) 542–552.
[9] E. Cocucci, F. Aguet, S. Boulant, T. Kirchhausen, The first five seconds in the life of a clathrin-coated pit, Cell 150 (2012) 495–507.
[10] S. de Keijzer, A. Sergé, F. van Hemert, P.H. Lommerse, G.E. Lamers, H.P. Spaink, T. Schmidt, B.E. Snaar-Jagalska, A spatially restricted increase in receptor mobility is involved in directional sensing during *Dictyostelium discoideum* chemotaxis, J. Cell Sci. 121 (2008) 1750–1757.
[11] F.M. Décaillot, M.A. Kazmi, Y. Lin, S. Ray-Saha, T.P. Sakmar, P. Sachdev, CXCR7/CXCR4 heterodimer constitutively recruits beta-arrestin to enhance cell migration, J. Biol. Chem. 286 (2011) 32188–32197.
[12] D. Dutta, J.G. Donaldson, Search for inhibitors of endocytosis: intended specificity and unintended consequences, Cell Logist. 2 (2012) 203–208.
[13] D. Dutta, C.D. Williamson, N.B. Cole, J.G. Donaldson, Pitstop 2 is a potent inhibitor of clathrin-independent endocytosis, PLoS ONE 7 (2012), e45799.
[14] M. Hamatake, T. Aoki, Y. Futahashi, E. Urano, N. Yamamoto, J. Komano, Ligand-independent higher-order multimerization of CXCR4, a G-protein-coupled chemokine receptor involved in targeted metastasis, Cancer Sci. 100 (2009) 95–102.
[15] G.S. Harms, L. Cognet, P.H.M. Lommerse, G.A. Blab, H. Kahr, R. Gamsjager, H.P. Spaink, N.M. Soldatov, C. Romanin, T. Schmidt, Single-molecule imaging of L-Type Ca2+ channels in live cells, Biophys. J. 81 (2001) 2639–2646.
[16] G.S. Harms, L. Cognet, P.H.M. Lommerse, G.A. Blab, T. Schmidt, Autofluorescent proteins in single-molecule research: applications to live cell imaging microscopy, Biophys. J. 80 (2001) 2396–2408.
[17] V. Jacquier, M. Prummer, J.-M. Segura, H. Pick, H. Vogel, Visualizing odorant receptor trafficking in living cells down to the single-molecule level, Proc. Natl. Acad. Sci. U. S. A. 103 (2006) (14325-12330).
[18] R.S. Kasai, A. Kusumi, Single-molecule imaging revealed dynamic GPCR dimerization, Curr. Opin. Cell Biol. 27 (2014) 78–86.
[19] R.H. Kim, B.D. Li, Q.D. Chu, The role of chemokine receptor CXCR4 in the biologic behavior of human soft tissue sarcoma, Sarcoma 2011 (2011) 593708.
[20] T. Kirchhausen, Imaging endocytic clathrin structures in living cells, Trends Cell Biol. 19 (2009) 596–605.
[21] P. Kleemann, D. Papa, S. Vigil-Cruz, R. Seifert, Functional reconstitution of the human chemokine receptor CXCR4 with G(i)/G (o)-proteins in Sf9 insect cells, Naunyn Schmiedeberg's Arch. Pharmacol. 378 (2008) 261–274.
[22] L. von Kleist, W. Stahlschmidt, H. Bulut, K. Gromova, D. Puchkov, M.J. Robertson, K.A. MacGregor, N. Tomilin, N. Tomlin, A. Pechstein, et al., Role of the clathrin terminal domain in regulating coated pit dynamics revealed by small molecule inhibition, Cell 146 (2011) 471–484.
[23] H. Kovar, Blocking the road, stopping the engine or killing the driver? Advances in targeting EWS/FLI-1 fusion in Ewing sarcoma as novel therapy, Expert Opin. Ther. Targets 18 (2014) 1315–1328.
[24] A. Levoye, K. Balabanian, F. Baleux, F. Bachelerie, B. Lagane, CXCR7 heterodimerizes with CXCR4 and regulates CXCL12-mediated G protein signaling, Blood 113 (2009) 6085–6093.
[25] Y. Lill, K.L. Martinez, M.A. Lill, B.H. Meyer, H. Vogel, B. Hecht, Kinetics of the initial steps of G protein-coupled receptor-mediated cellular signaling revealed by single-molecule imaging, ChemPhysChem 6 (2005) 1633–1640.
[26] P.H.M. Lommerse, G.A. Blab, L. Cognet, G.S. Harms, E.B. Snaar-Jagalska, H.P. Spaink, T. Schmidt, Single-molecule imaging of lipid-anchored proteins reveals domains in the cytoplasmic leaflet of the cell membrane, Biophys. J. 86 (2004) 609.
[27] K.E. Luker, M. Gupta, G.D. Luker, Imaging chemokine receptor dimerization with firefly luciferase complementation, FASEB J. 23 (2009) 823–834.
[28] C. Luo, H. Pan, M. Mines, K. Watson, J. Zhang, G.H. Fan, CXCL12 induces tyrosine phosphorylation of cortactin, which plays a role in CXC chemokine receptor 4-mediated extracellular signal-regulated kinase activation and chemotaxis, J. Biol. Chem. 281 (2006) 30081–30093.
[29] S. Mangmool, H. Kurose, G(i/o) protein-dependent and -independent actions of Pertussis Toxin (PTX), Toxins Basel 3 (2011) 884–899.
[30] D. Massotte, G protein-coupled receptor overexpression with the baculovirus-insect cell system: a tool for structural and functional studies, Biochim. Biophys. Acta 1610 (2003) 77–89.
[31] A. Martínez-Ramírez, S. Rodríguez-Perales, B. Meléndez, B. Martínez-Delgado, M. Urioste, J.C. Cigudosa, J. Benítez, Characterization of the A673 cell line (Ewing tumor) by molecular cytogenetic techniques, Cancer Genet. Cytogenet. 141 (2003) 138–142.
[32] A.S. Martins, J.L. Ordóñez, A.T. Amaral, F. Prins, G. Floris, M. Debiec-Rychter, P.C. Hogendoorn, E. de Alava, IGF1R signaling in Ewing sarcoma is shaped by clathrin-/caveolin-dependent endocytosis, PLoS ONE 6 (2011), e19846.
[33] H.T. McMahon, E. Boucrot, Molecular mechanism and physiological functions of clathrin-mediated endocytosis, Nat. Rev. Mol. Cell Biol. 12 (2011) 517–533.
[34] T. Meckel, S. Semrau, M.J.M. Schaaf, T. Schmidt, Robust assessment of protein complex formation in vivo via single-molecule intensity distributions of autofluorescent proteins, J. Biomed. Opt. 16 (2011) 076016.
[35] J. Moss, P. Bruni, J.A. Hsia, S.C. Tsai, P.A. Watkins, J.L. Halpern, D.L. Burns, Y. Kanaho, P.P. Chang, E.L. Hewlett, Pertussis toxin-catalyzed ADP-ribosylation: effects on the coupling of inhibitory receptors to the adenylate cyclase system, J. Recept. Res. 4 (1984) 459–474.
[36] W. Mueller, D. Schütz, F. Nagel, S. Schulz, R. Stumm, Hierarchical organization of multi-site phosphorylation at the CXCR4 C terminus, PLoS ONE 8 (2013), e64975.
[37] U. Naumann, E. Cameroni, M. Pruenster, H. Mahabaleshwar, E. Raz, H.G. Zerwes, A. Rot, M. Thelen, CXCR7 functions as a scavenger for CXCL12 and CXCL11, PLoS ONE 5 (2010), e9175.
[38] S. Otsuka, G. Bebb, The CXCR4/SDF-1 chemokine receptor axis: a new target therapeutic for non-small cell lung cancer, J. Thorac. Oncol. 3 (2008) 1379–1383.
[39] L. Pelkmans, A. Helenius, Endocytosis via caveolae, Traffic 3 (2002) 311–320.
[40] N. Papadopoulou, E.A. Papakonstanti, G. Kallergi, K. Alevizopoulos, C. Stournaras, Membrane androgen receptor activation in prostate and breast tumor cells: molecular signaling and clinical Impact, IUBMB Life 61 (2009) 56–61.
[41] M. Rey, A. Valenzuela-Fernández, A. Urzainqui, M. Yáñez-Mó, M. Pérez-Martínez, P. Penela, F. Mayor Jr., F. Sánchez-Madrid, Myosin IIA is involved in the endocytosis of CXCR4 induced by SDF-1alpha, J. Cell Sci. 120 (2007) 1126–1133.
[42] S.L. Ritter, R.A. Hall, Fine-tuning of GPCR activity by receptor-interacting protein, Nat. Rev. Mol. Cell Biol. 10 (2009) 819–830.
[43] J.B. Rubin, Chemokine signaling in cancer: one hump or two? Semin. Cancer Biol. 19 (2009) 116–122.
[44] M. Sáinz-Jaspeado, L. Lagares-Tena, J. Lasheras, F. Navid, C. Rodriguez-Galindo, S. Mateo-Lozano, V. Notario, X. Sanjuan, X. Garcia Del Muro, A. Fabra, O.M. Tirado, Caveolin-1 modulates the ability of Ewing's sarcoma to metastasize, Mol. Cancer Res. 8 (2010) 1489–1500.
[45] M. Sáinz-Jaspeado, J. Huertas-Martinez, L. Lagares-Tena, J. Martin Liberal, S. Mateo-Lozano, E. de Alava, C. de Torres, J. Mora, X.G. Del Muro, O.M. Tirado, EphA2-induced angiogenesis in ewing sarcoma cells works through bFGF production and is dependent on caveolin-1, PLoS ONE 8 (2013), e71449.
[46] J. Samaj, F. Baluska, B. Voigt, M. Schlicht, D. Volkmann, D. Menzel, Endocytosis, actin cytoskeleton, and signaling, Plant Physiol. 135 (2004) 1150–1161.
[47] L.G.L. Sand, K. Scotlandi, D. Berghuis, B.E. Snaar-Jagalska, P. Picci, T. Schmidt., K. Szuhai, P.C.W. Hogendoorn, CXCL14, CXCR7 expression and CXCR4 splice variant ratio associated with survival and metastasis in Ewing sarcoma patients, Eur. J. Cancer (2015).

[48] M.J. Saxton, Lateral diffusion in an archipelago single-particle diffusion, Biophys. J. 64 (1993) 1766–1780.
[49] T. Schmidt, G.J. Schütz, W. Baumgartner, H.J. Gruber, H. Schindler, Imaging of single molecule diffusion, Proc. Natl. Acad. Sci. U. S. A. 93 (1996) 2926–2929.
[50] V. Schwartz, A. Krüttgen, J. Weis, C. Weber, T. Ostendorf, H. Lue, J. Bernhagen, Role for CD74 and CXCR4 in clathrin-dependent endocytosis of the cytokine MIF, Eur. J. Cell Biol. 91 (2012) 435–449.
[51] S. Semrau, T. Schmidt, Particle image correlation spectroscopy (PICS): retrieving nanometer-scale correlations from high-density single-molecule position data, Biophys. J. 92 (2007) 613–621.
[52] A. Serge, S. de Keijzer, F. Van Hemert, M.R. Hickman, D. Hereld, H.P. Spaink, T. Schmidt, B.E. Snaar-Jagalska, Quantification of GPCR internalization by single-molecule microscopy in living cells, Integr. Biol. 3 (2011) 675–683.
[53] J.Y. Springael, E. Urizar, M. Parmentier, Dimerization of chemokine receptors and its functional consequences, Cytokine Growth Factor Rev. 16 (2005) 611–623.
[54] A.D. Stuart, T.D. Brown, Entry of feline calicivirus is dependent on clathrin-mediated endocytosis and acidification in endosomes, J. Virol. 80 (2006) 7500–7509.
[55] B.A. Teicher, S.P. Fricker, CXCL12 (SDF-1)/CXCR4 pathway in cancer, Clin. Cancer Res. 16 (2010) 2927–2931.
[56] O.M. Tirado, S. Mateo-Lozano, J. Villar, L.E. Dettin, A. Llort, S. Gallego, J. Ban, H. Kovar, V. Notario, Caveolin-1 (CAV1) is a target of EWS/FLI-1 and a key determinant of the oncogenic phenotype and tumorigenicity of Ewing's sarcoma cells, Cancer Res. 66 (2006) 9937–9947.
[57] P. Tsao, T. Cao, M. von Zastrow, Role of endocytosis in mediating downregulation of G-protein-coupled receptors, Trends Pharmacol. Sci. 22 (2001) 91–96.
[58] M. Ueda, Y. Sako, T. Tanaka, P. Devreotes, T. Yanagida, Single-molecule analysis of chemotactic signaling in *Dictyostelium* cells, Science 294 (2001) 864–867.
[59] F. van Hemert, M.D. Lazova, B.E. Snaar-Jagaska, T. Schmidt, Mobility of G proteins is heterogeneous and polarized during chemotaxis, J. Cell Sci. 123 (2010) 2922–2930.
[60] E.V. Vassilieva, A. Nusrat, Vesicular trafficking: molecular tools and targets, Methods Mol. Biol. 440 (2008) 3–14.
[61] S. Venkatesan, J.J. Rose, R. Lodge, P.M. Murphy, J.F. Foley, Distinct mechanisms of agonist-induced endocytosis for human chemokine receptors CCR5 and CXCR4, Mol. Biol. Cell 14 (2003) 3305–3324.
[62] A.J. Vila-Coro, J.M. Rodríguez-Frade, A. Martín De Ana, M.C. Moreno-Ortíz, C. Martínez-A, M. Mellado, The chemokine SDF-1alpha triggers CXCR4 receptor dimerization and activates the JAK/STAT pathway, FASEB J. 13 (1999) 1699–1710.
[63] L.H. Wang, K.G. Rothberg, R.G. Anderson, Mis-assembly of clathrin lattices on endosomes reveals a regulatory switch for coated pit formation, J. Cell Biol. 123 (1993) 1107–1117.
[64] B. Wu, E.Y. Chien, C.D. Mol, G. Fenalti, W. Liu, V. Katritch, R. Abagyan, A. Brooun, P. Wells, F.C. Bi, D.J. Hamel, P. Kuhn, T.M. Handel, V. Cherezov, R.C. Stevens, Structures of the CXCR4 chemokine GPCR with small-molecule and cyclic peptide antagonists, Science 330 (2010) 1066–1071.
[65] D. Yarar, C.M. Waterman-Storer, S.L. Schmid, A dynamic actin cytoskeleton functions at multiple stages of clathrin-mediated endocytosis, Mol. Biol. Cell 16 (2005) 964–975.
[66] F. Ye, D.K. Breslow, E.F. Koslover, A.J. Spakowitz, W.J. Nelson, M.V. Nachury, Single molecule imaging reveals a major role for diffusion in the exploration of ciliary space by signaling receptors, eLife 2 (2013), e00654.